Scientia Iranica A (2014) 21(4), 1217–1230

Sharif University of Technology
Scientia Iranica
Transactions A: Civil Engineering
www.scientiairanica.com

Effect of turbulence closure models on the accuracy of moving particle semi-implicit method for the viscous free surface flow

M. Kolahdoozan*, M.S. Ahadi and S. Shirazpoor

Department of Civil and Environmental Engineering, Amirkabir University of Technology, Tehran, Iran.

Received 30 June 2012; received in revised form 8 August 2013; accepted 22 February 2014

KEYWORDS
Lagrangian;
Turbulence;
Mixing length theory;
$k-\varepsilon$ model;
MPS method;
Incomplete conjugate cholesky gradient.

Abstract. The purpose of this paper is to put forward the effect of different turbulence closure models on an enhanced Moving Particle Semi-implicit (MPS) method for solving continuity and momentum equations of viscous fluid. MPS method is a mesh-free Lagrangian method capable of solving non-linear governing equations and simulating complex free surface flow circumstances. Various turbulence closure models are added to a MPS program and applied it to different fluid mechanic problems to investigate the effect of these types of closure. Dam break simulation outcome indicates that the two-equation $k-\varepsilon$ turbulence model improves free surface estimation accuracy most. It also shows that type of utilized Kernel function has no significant efficacy on stability when the effect of turbulence is included. Further, an algorithm called Incomplete Conjugate Cholesky Gradient (ICCG) is applied for computing pressure implicitly. Applying developed model to well-known sample problems cited in the literature represents that using turbulence closure models can enhance the prediction of developed model as well as stability of the simulations.

1. Introduction

In response to the need for estimating free surface flow in many industrial and natural problems, the application of numerical methods is significantly increasing. Many investigations are performed in the field of determining free surface flow and as a result, different numerical methods are proposed. Among Eulerian methods, the single-phase and two-phase VOF can be named. Ashigriz and Poo [1] developed single-phase VOF model for estimating hydrodynamic parameters. This model was later extended by Van der meer [2] and resulted in SKYLLA which is a model based on VOF combined with an algorithm of second order accuracy. Also, the two-phase VOF model was proposed by Hieu and Tanimoto [3]. Despite the improvements of VOF method, numerical dispersion of this method seems inevitable [2].

Due to the insufficient flexibility of Eulerian methods in solving problems with high deformation, moving boundary conditions and complex geometry, meshless methods were mostly used as replacement to mesh-based methods in recent years. Among these mesh-free methods, the Mesh-free Particle Methods (MPMs) are more common in fluid mechanics problems.

In 1977, the Lagrangian Smoothed Particle Hydrodynamics (SPH) method was proposed by Lucy [4] and later extended by Gingold and Monaghan [5] for solving astrophysics problems. Monaghan presented the general form of SPH method for incompressible fluid [6]. In spite of its early appearance, the method

*. *Corresponding author. Tel.: +98 21 64543023; Fax: +98 21 66414213*
E-mail addresses: mklhdzan@aut.ac.ir (M. Kolahdoozan); mina_ahadi@aut.ac.ir (M.S. Ahadi); samina_2025@yahoo.com (S. Shirazpoor)

did not attract the interest of researchers in other fields until the beginning of the 1990s, when the method was successfully applied in fields, such as impact penetration in solids [7,8] and two-phase flow [9]. In the particular case of fluid dynamics, perhaps the most important success of the meshless SPH technique was the application of the method to free-surface flows [10], first attempted by Monaghan [11]. Monaghan also studied the behavior of gravity currents and solitary wave [12,13], the wave arrival at a beach [14] or the behavior of a Scott Russell's wave generator [15]. The unique characteristic of SPH methods lies in creating a harmonious combination of the Lagrangian formulations and particle approximation. In other words, the SPH particles not only function as interpolating points, but also carry the properties of particles. In this method, diffusion terms are calculated. Of course, this method suffers from several disadvantages such as low accuracy, difficulty in enforcing essential boundary conditions, and tensile instability which the latter is due to its low accuracy [16].

Another famous Lagrangian method is Moving Particle Semi-implicit (MPS). This method is basically the modified form of particle method proposed by Koshizuka and Oka [17]. This method represented an agreeable result in applying to non-viscous problems of wave interaction and thus attracted the interest of fluid dynamics researchers [18].

In the MPS method, the fluid is divided into several moving particles and diffusion terms are calculated during the motion of these particles. Therefore, the usual numerical diffusion problem in Eulerian methods does not take place. In this method, incompressibility is presented by keeping the density of particles constant during the computational time. In particle methods such as MPS, the equations of continuity and momentum are converted into equations of interaction between particles in which all interactions are limited to a specific distance and weighing of interaction between two particles with distance of r is determined based on Kernel function. The movement of each particle due to the interaction of neighboring particles is calculated using Kernel weighing function approximation. Consequently, Laplacian, gradient and divergence operators change to consider the effect of moving particles. Different Kernel functions and methods are proposed for solving Poisson pressure equation that resulted in more stability and accuracy of MPS method. Atai-Ashtiani and Farhadi [19] comprised the effect of using different Kernel functions in dam break problem.

Different studies indicate that stability of this method is more than SPH method [19]. However, the current method suffers from instability and inaccuracy problems, too. Many approaches were proposed in order to enhance stability and accuracy of MPS. Khayyer and Gotoh [18] obtained a more stable solution for this numerical method called CMPS by using the modified form of gradient term. In addition a higher order Laplacian model which enhances stabilization of pressure calculation due to their test cases was proposed [20]. Kondo and Koshizuka attained smoother pressure distributions by decreasing unphysical numerical oscillations using a new formulation for the source term of Poisson equation of pressure [21].

MPS is capable of modeling free surface of inviscid incompressible fluids, and analyzing problems with high continuous interaction of fluid-structure. Among application of MPS method are dam breaking type problem, wave breaking and its interaction with floating rigid unit, collapsing water droplet and interaction of fluid with elastic structure [22], solitary wave breaking on mild slopes [23], bubble condensation [24], an extremely nonlinear phenomenon such as shipping water [25], problems with open-boundary [26] and highly deformed free surface and spray generated by planning of a high-speed boat [27]. Effect of turbulence is not considered in MPS models, yet [17,19,22].

In this research study, MPS method is extended for estimating free surface of turbulent fluid flow. In the present method, the effect of turbulence is included using two turbulence models of $k-\varepsilon$ and Prandtl's mixing length theory. The developed model is based on the MPS model which was developed by Fayyaz and Kolahdoozan [28]. Equations have been updated to latest achievements by Khayyer and Gotoh [18] in order to provide more stability and accuracy. In this paper, the effect of turbulence is demonstrated on more accurate estimation of free surface using Prandtl's mixing length theory, and through comparing the results with those of constant viscosity. Besides, the two equations of $k-\varepsilon$ turbulence model, based on the Lagrangian method of SPH [29], are applied to MPS method successfully.

Since in previous research studies it was stated that the type of Kernel function is effective in the stability of MPS method for modeling inviscid fluids [19], in the current study the effect of Kernel functions on stability of developed model is investigated in the presence of turbulence. According to the developed model, the results of dam breaking problem indicate that in this case, the type of Kernel function used in MPS model has no effect on stability.

In MPS method, equations are solved implicitly, and for increasing the convergence it was combined with projection method. Therefore, its computational speed is more than other similar models of estimating free surface flow. An algorithm called Incomplete Conjugate Cholesky Gradient (ICCG) was applied to compute the pressure implicitly to enhance the stability. ICCG is a numerical solution for linear system of equations. The pressure results of numerical examples show the effect of utilizing this algorithm.

2. Governing equations of MPS method

Governing equations of viscous fluid flow include continuity and momentum equations which can be represented as follows [30]:

$$\begin{cases} \frac{1}{\rho}\frac{D\rho}{Dt} + \nabla.\vec{u} = 0 \\ \\ \frac{D\vec{u}}{Dt} = -\frac{1}{\rho}\nabla P + \frac{1}{\rho}\nabla.\vec{\tau} + \vec{f} \end{cases} \quad (1)$$

where $\vec{u}$ is the velocity vector, t is time, ρ is fluid density, P is pressure, υ_t is eddy viscosity, and f is the vector of body forces, impact force of particles and surface tension.

While in the Eulerian methods the pressure is considered as two separate terms of static and dynamic, in this method the pressure term can be considered as a dependent variable containing the amounts of static and dynamic terms together. This is because in the MPS method, the free surface flow is computed automatically for each particle. Thus, by adding Poisson pressure equation, the pressure term can be calculated for all particles. The Poisson equation is written as [17]:

$$\left(\nabla^2 P\right)_i^{k+1} = \frac{\rho}{(\Delta t)^2}\frac{n_i^k - n_0}{n_0}, \quad (2)$$

where p is the sum of static and dynamic pressures, ρ is the fluid density, t is the time variable, and k is the step of calculation.

In the above equations, n_i is the density of particle i at location n_i which is defined as:

$$n_i = \sum_{i \neq j} w\left(|r_j - r_i|\right) \qquad \vec{r_i} = x\vec{i} + y\vec{j}. \quad (3)$$

Also, the standard density n_0 and the λ coefficient are defined as:

$$n_0 = \int_V w(r)dV, \quad (4)$$

$$\lambda = \frac{\sum\limits_{j \neq i} w(r_j - r_i)|r_j - r_i|^2}{\sum\limits_{j \neq i} w(r_j - r_i)}. \quad (5)$$

For considering the interaction of each particle with its neighboring particles in MPS method, Eqs. (1) are discretized.

To obtain a gradient vector, the operator of gradient between the particle i and its neighboring particles j is averaged using the Kernel weighing function:

$$(\nabla\phi)_i = \frac{d}{n_0}\sum_{i \neq j}\frac{\phi_j - \phi_i}{|r_j - r_i|^2}(r_j - r_i)w\left(|r_j - r_i|\right), \quad (6)$$

where ϕ is the calculated amount in model, d is the number of dimensions (e.g. 2, 3), n_0 is the number density, r is the vector location of particle, and $w(r)$ is the Kernel function. Applying modifications in gradient model, Khayyer and Gotoh [18] obtained more stable solution for this numerical method called CMPS.

For determining ϕ_i in Eq. (3), ϕ_i' is applied which is the minimum amount of ϕ between neighboring particles in the efficient radius r_e:

$$(\nabla\phi)_i = \frac{d}{n_0}\sum_{i \neq j}\frac{(\phi_i + \phi_j) - (\phi_i' + \phi_j')}{|r_j - r_i|^2}$$

$$(r_j - r_i)w\left(|r_j - r_i|\right). \quad (7)$$

The Laplacian operator is written as [17]:

$$(\nabla^2\phi)_i = \frac{2d}{\lambda n_0}\sum_{i \neq j}(\phi_i - \phi_j)w\left(|r_j - r_i|\right). \quad (8)$$

The presented Laplacian formula is in a conservative form, because the amount separated from particle i will be attracted by particle j.

In MPS method the equations of continuity and momentum are converted to interaction equations of particles using different operators. All interactions between particles are limited to a specific distance known as efficient radius. The weighing of different neighboring particles within efficient radius on the desired particle is calculated based on Kernel functions in which r is the distance between two particles, i and j, and r_e is the efficient radius of Kernel function.

Atai-Ashtiani and Farhadi [19] investigated the effect of six Kernel functions on stability of single-phase MPS method through modeling the dam breaking problem. These Kernel functions are presented in Table 1. According to their conclusions, the Kernel function proposed by Shao and Lo [31] yielded the best stability for MPS method. In this paper, a similar approach is used in the presence of turbulence closures and the effect of these Kernel functions on the stability of MPS method is investigated through modeling a dam breaking problem.

3. Turbulence models

Since the fluid investigated in this study is viscous and the flow is turbulent, two turbulence models of Prandtl's mixing length theory and $k-\varepsilon$ closure models are deployed for determining the fluid eddy viscosity.

The first turbulence model which provided a distribution for eddy viscosity was provided by Prandtl (1925) known as the Prandtl's mixing length theory and originates from the dynamic theory of gases. The Prandtl's mixing length theory was widely applied in

Table 1. Different Kernel functions used in MPS method (Atai-Ashtiani and Farhadi, 2006) [19].

Reference	Formula	Function
Belyschko et al. (1996)	$w(r)=\begin{cases} e^{-(r/\alpha r_e)^2} & 0\le r\le r_e \\ 0 & r_e<r \end{cases}$	KF1
Violeau et al. (2007)	$w(r)=\frac{96}{1199}\pi\begin{cases} \left(\frac{5}{2}-\frac{r}{r_e}\right)^4-5\left(\frac{3}{2}-\frac{r}{r_e}\right)^4+10\left(\frac{1}{2}-\frac{r}{r_e}\right)^4 & 0\le r\le \frac{r_e}{2} \\ \left(\frac{5}{2}-\frac{r}{r_e}\right)^4-5\left(\frac{3}{2}-\frac{r}{r_e}\right)^4 & \frac{r_e}{2}\le r\le \frac{3}{2}r_e \\ \left(\frac{5}{2}-\frac{r}{r_e}\right)^4 & \frac{3}{2}r_e\le r\le \frac{5}{2}r_e \\ 0 & r_e<r \end{cases}$	KF2
Belyschko et al. (1996)	$w(r)=\begin{cases} 1-6\left(\frac{r}{r_e}\right)^2+8\left(\frac{r}{r_e}\right)^3-3\left(\frac{r}{r_e}\right)^4 & 0\le r\le r_e \\ 0 & r_e<r \end{cases}$	KF3
Koshizuka and Oka (1996)	$w(r)=\begin{cases} -2\left(\frac{r}{r_e}\right)^2+2 & 0\le r\le \frac{r_e}{2} \\ \left(2\frac{r}{r_e}-2\right)^2 & \frac{r_e}{2}\le r\le r_e \\ 0 & r_e\le r \end{cases}$	KF4
Oak institute	$w(r)=\begin{cases} \frac{r}{r_e}-1 & 0\le r\le r_e \\ 0 & r_e\le r \end{cases}$	KF5
Shao and Lo (2003)	$w(r)=\begin{cases} \frac{40}{7\pi r_e^2}\left(1-6(\frac{r}{r_e})^2+6(\frac{r}{r_e})^3\right) & 0\le r\le \frac{r_e}{2} \\ \frac{40}{7\pi r_e^2}\left(2-2\frac{r}{r_e}\right)^3 & \frac{r_e}{2}<r<r_e \\ 0 & r_e<r \end{cases}$	KF6

estuaries and coastal waters. According to this theory the eddy viscosity is written as [32]:

$$\upsilon_t = k u_* z \left(1-\frac{z}{H}\right). \tag{9}$$

In the derivation of Eq. (9), the assumption of logarithmic velocity profile was used. In MPS method, the eddy viscosity for each particle is obtained based on Prandtl's mixing length theory as:

$$\upsilon_{t,i} = k u_{*i} z_i \left(1-\frac{z_i}{H}\right). \tag{10}$$

Also for enforcing the effect of turbulence in MPS method, the well-known $k-\varepsilon$ equations are deployed in the developed model.

First, for each particle such as i, a turbulence kinetic energy, k_i, and energy dissipation rate, ε_i, are defined. Based on the $k-\varepsilon$ equations, we have:

$$\upsilon_{t,i} = c_\mu \frac{k_i^2}{\varepsilon_i}. \tag{11}$$

The equation governing the variation of turbulence kinetic energy can be shown to be as [26]:

$$\frac{dk}{dt} = P-\varepsilon+\nabla.\left[\left(\upsilon+\frac{\upsilon_t}{\sigma_k}\right)\nabla k\right]. \tag{12}$$

This equation is analogous to the convection-diffusion equation where the producing term of kinetic energy, P, is similar to the source term, and the term of energy dissipation, ε, is similar to the sink term. Therefore, in the MPS method the convection equation, k, is written as:

$$\frac{\Delta k}{\Delta t} = P_i-\varepsilon_i+\frac{\upsilon_{k.i}2d}{\lambda n_0}.\sum(k_j-k_i).w\left(|r_{ij}|\right), \tag{13}$$

where:

$$\upsilon_{k.i} = \upsilon+\nu_{t.i}/\sigma_k. \tag{14}$$

The source term is defined as $P=-R_{ij}S_{ij}$ [26]:

$$\vec{R} = \frac{2}{3}k\vec{I}-2\upsilon_t\vec{S} \quad \Rightarrow \quad P=\upsilon_t S^2, \tag{15}$$

where $\vec{R}$ is the Reynolds stresses according to the Bousinesq Theorem, and $\vec{S}$ is the mean values of strain tensor.

However, for preventing any overestimation of k in cases with high rates of strain variation (such as impact of water to a breakwater), it should be noted that the non-isotropic turbulence will be limited by $c_\mu^{1/2}$. Therefore, for high deformations a linear strain variation rate is considered in this study, and the source term of particle i is limited as:

$$P_i = \text{Min}\left(\sqrt{c_\mu}, c_\mu S_i \frac{k_i}{\varepsilon_i}\right) k_i S_i. \tag{16}$$

For estimating the rate of strain S_i, one can write [30]:

$$S_i = \frac{1}{2}\left(\frac{\partial u_i}{\partial y} + \frac{\partial v_i}{\partial x}\right), \tag{17}$$

where its MPS form can be presented as:

$$S_i = \frac{d}{2n_0}\sum_{i\neq j}\frac{u_i u_j}{(x_i x_j)^2 + (y_i y_j)^2}(x_i x_j) w\left(|r_i r_j|\right) + \sum_{i\neq j}\frac{v_i v_j}{(x_i x_j)^2 + (y_i y_j)^2}(y_i y_j) w\left(|r_i r_j|\right). \tag{18}$$

Thus, when S_i, k_i, ε_i and c_μ are given, the source term of $k-\varepsilon$ equation can be determined. Therefore, in $k-\varepsilon$ model the k_i can be computed using Eq. (12).

The energy dissipation rate, ε, is written as:

$$\frac{d\varepsilon}{dt} = \nabla.\left(\upsilon + \frac{\upsilon_t}{\sigma_\varepsilon}\nabla\varepsilon\right) + \frac{\varepsilon}{k}(C_{\varepsilon,1}P - C_{\varepsilon,2}\varepsilon), \tag{19}$$

where its MPS form can be presented as:

$$\frac{\Delta\varepsilon}{\Delta t} = \frac{\upsilon_{\varepsilon,i} 2d}{\lambda n_0}.\sum(\varepsilon_j - \varepsilon_i).w(|r_{ij}|) + \frac{\varepsilon_i}{k_i}(C_{\varepsilon,1}P_i - C_{\varepsilon,2}\varepsilon_i), \tag{20}$$

in which:

$$\upsilon_{\varepsilon.i} = \upsilon + \nu_{t.i}/\sigma_\varepsilon. \tag{21}$$

In this study, the constant coefficient proposed by Launder and Spaulding are deployed [26]:

$$c_\mu = 0.09, \quad \sigma_k = 1.0, \quad \sigma_\varepsilon = 1.0,$$

$$C_{\varepsilon,1} = 1.44, \quad C_{\varepsilon,2} = 1.92, \quad \upsilon \approx 0.$$

4. Numerical solution procedure

In the developed MPS model, the equations were written for two consecutive time steps. Also, the projection method is applied to enhance the convergence speed which separates the solution of advection and diffusion terms in Navier-Stokes equations. Hence, solution of Navier-Stokes equations will be divided into two completely different half time steps. While, in first half time step, the equations are solved in the presence of viscosity and gravitational terms; in the second time step the results obtained in the previous time step will be modified in the presence of remaining terms of Navier-Stokes equations including pressure gradient, impact force of particles, surface tension, etc. Based on the projection method, in the first half time step the Navier-Stokes equations are considered as [17]:

$$\frac{D\bar{u}}{Dt} = \upsilon_t \nabla^2 \bar{u} + \bar{g}. \tag{22}$$

To solve Eq. (22), first eddy viscosity should be computed.

In Prandtl's mixing length theory the turbulence eddy viscosity, υ_t, is computed based on the velocity, u, and location of the particle, z, as:

$$\upsilon_{t,i} = k u_{*i} z_i \left(1 - \frac{z_i}{H}\right). \tag{23}$$

In the two-equation $k-\varepsilon$ turbulence model, the solution algorithm for each time step is as follows:

1. Determining the initial k and ε at first time step;
2. Determining the source term P_i of $k-\varepsilon$ equation after calculating S_i;
3. Calculating the turbulence kinetic energy, k_i;
4. Calculating the coefficient of energy dissipation, ε_i;
5. Calculating the turbulence eddy viscosity of particle as $\upsilon_{t,i} = c_\mu \frac{k_i^2}{\varepsilon_i}$.

After determining the turbulence eddy viscosity and computing velocity variations, $\nabla\bar{u}$, through solution of equations, the necessary corrections can be enforced on velocity and location of particles, given by:

$$\bar{u^*} = \Delta\bar{u^*} + \bar{u^t}, \qquad \bar{r^*} = \Delta\bar{r^*} + \bar{r^t}, \tag{24}$$

with $\bar{u^t}$ and $\bar{r^t}$ being velocity and location of the particle at time t, respectively. Also $\bar{u^*}$ and $\bar{r^*}$ are velocity and location of the particles at the time * or $t + 1/2$.

Given the new velocity and location of each particle, the second step of projection method will be performed through implicit solution of pressure Poisson equation and obtaining new values of pressure for each particle as:

$$p_i^{t+1} = \frac{\lambda n_0}{2d\sum\limits_{i\neq j} w(|r_{ij}|)}\left[\frac{2d}{\lambda n_0}\sum_{i\neq j} p_j^t w(|r_{ij}|) + \frac{\rho}{\Delta t^2}\frac{n_i^{t+1/2} - n_0}{n_0}\right], \tag{25}$$

in which t and $t+1$ represent the current and next time steps, respectively. In this equation, which is derived from Eq. (2) and discretized using Eq. (5), the first right-hand side term represents the weight-averaged pressure at current time step. Also, the second right-hand side term represents the density deviation of particle from its current amount at next time step. This density deviation is created due to correcting the location of particles. Therefore, with density correction in the form of an effect on pressure, the continuity equation will be satisfied. This is because the Pressure Poisson equation is derived from both continuity and momentum equations. Discretization using Laplacian formula of MPS (Eq. (5)) leads to a linear $N \times N$ system of equations, with N being the number of particles, that needs to be solved by one of the iterative procedures. Pressure Poisson equation is solved via ICCG method and the obtained pressure is used to solve the momentum equation implicitly. By using this semi-implicit algorithm, the stability of pressure due to the change of particle density is well improved and the stable pressure was obtained in dam-break simulation by Shao and Lo [31] who deployed this method for the solution of system of equation in SPH method [13].

To solve the linear system of algebraic equations, the Cholesky decomposition was deployed. A as a symmetric positive definite matrix in the system of linear equation, $Ax = b$, can be decomposed into two lower-triangular $[L]$ and upper-triangular $[L]^T$ matrixes which are transpose of each other as:

$$[A] = [L][L]^T, \tag{26}$$

$$[L][L]^T[X] = [b]. \tag{27}$$

Introducing the virtual matrix $[Y]$ and solving following linear system of equations, $[Y]$ values can be obtained using the equation:

$$[L][Y] = [b]. \tag{28}$$

Afterwards, using the virtual matrix, the linear system of equation performing with upper-triangular matrix is calculated and $[X]$ values are gained as:

$$[L]^T[X] = [Y]. \tag{29}$$

Finally, given the velocity values and location at time step * or $t+1/2$ and also the pressure for each particle, one can enforce the correction resulted from the deviation of particle density at the second step of projection method. This correction is enforced with solving the Navier-Stokes equations. The main remaining term in Navier-Stokes equation is the pressure gradient. In the second phase of projection method we use:

$$\rho \frac{D\bar{u}}{Dt} = -\nabla p + \bar{\delta}_{\mathrm{gl}} + \frac{\sigma k' \delta_{\mathrm{st}}}{\rho} \bar{n}, \tag{30}$$

where σ denotes the coefficient of surface tension, k' is the surface curvature, $\bar{n}$ is the unit surface vector perpendicular to the surface, and δ_{st} is the delta function with $\delta_{\mathrm{st}} = 1$ for surface particles and $\delta_{\mathrm{st}} = 0$ for other particles.

Through implicit solution of Eq. (30), velocities can be obtained. Consequently, the location of particles can be corrected so that the continuity and momentum equations are satisfied as:

$$\bar{u}^{t+1} = \Delta\bar{u} + \bar{u}^*, \qquad \bar{r}^{t+1} = \Delta\bar{u}.dt + \bar{r}^*. \tag{31}$$

The solution algorithm can be briefly divided into three sections:

1. The first phase of projection and correcting the locations;
2. Solving the pressure Poisson equation and obtaining pressures;
3. The second phase of projection and correcting locations and velocities (enforcing the pressure values).

5. Results and analysis

To represent the effect of turbulence modeling in improving the MPS model results, first the dam break problem is chosen. This problem is solved by many researchers through different Eulerian and Lagrangian methods. To represent the enhancement of the developed model regarding its stability point of view, the Scott Russell wave generator and wave run-up are then modeled.

5.1. Dam break problem

The first problem for investigating the applicability of developed model and also the efficiency of incorporated algorithms, a dam break problem is chosen for modeling purposes. The schematic view of the problem is shown in Figure 1.

The basic variables, such as initial distance between particles, dr, time step, dt, and efficient radius, r_e, have their own optimum values based on problem

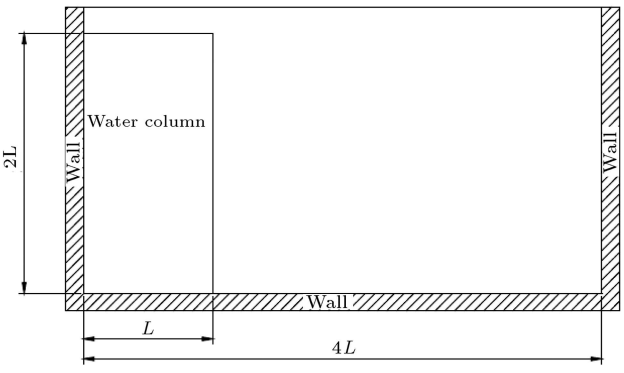

Figure 1. Geometry of dam break problem.

conditions and Courant number. In dam break problem the Courant number is written as [29]:

$$C_r = \frac{dt|u|}{dr} \leq 0.2. \quad (32)$$

Here, the values of $dt = 0.003$, $dr = 0.016$ and $r_e = 1.6$ m are selected based on the computation of numerical and empirical profiles and nature of free surface in dam break problems [29].

Consequently, the dam break problem is solved by MPS method and using turbulence closures, such as Prandtl's mixing length theory and two-equation $k-\varepsilon$ model. The model results are compared with three sets of results presented in Figures 2 and 3.

The first set of results is experimental data of Koshizuka (1996) which are available only for 1 second of breaking process [17]. The second and third sets of results are numerical results of inviscid fluid and fluid with constant viscosity, respectively [29].

The results of comparisons indicate that by using Prandtl's mixing length theory and two-equation $k-\varepsilon$ model, the estimation of free surface flow was improved. In Figure 4, comparison is made for model results with experimental values for different turbulence closure models at $t = 0.6$ s. According to Figure 4, the non-viscous model has the maximum error of $\sim 9\%$ among the other models. In contrast, the two-equation $k-\varepsilon$ model has achieved the minimum error of less than 1%.

Moreover, a comparison is made for the number of particles in free surface flow (i.e. those with atmospheric pressure) for different time steps. The basis of this comparison is that the less the number of free surface particles indicates better and smoother free surface flow modeling (Figure 5).

In Figure 5 the horizontal axis represents the time and the vertical axis represents the number of particles which are in free surface flow (i.e. those with atmospheric pressure). Comparison of these methods reveals that using the Prandtl's mixing length theory and two-equation $k-\varepsilon$ model, the estimation of free surface flow is improved. This improvement in accuracy of MPS method, when using Prandtl's mixing length theory, is due to determining the eddy viscosity of each particle in each time step based on their location and velocity at the specified time step. Also, this is due to determining the eddy viscosity in each time step when using $k-\varepsilon$ equations. Besides, the accuracy of model is improved due to calculating the interaction between fluid and air phases.

Atai-Ashtiani and Farhadi [19] stated that the type of Kernel function is effective in the stability of MPS method for modeling inviscid flows (i.e. fluids without turbulence). Therefore, the effect of Kernel

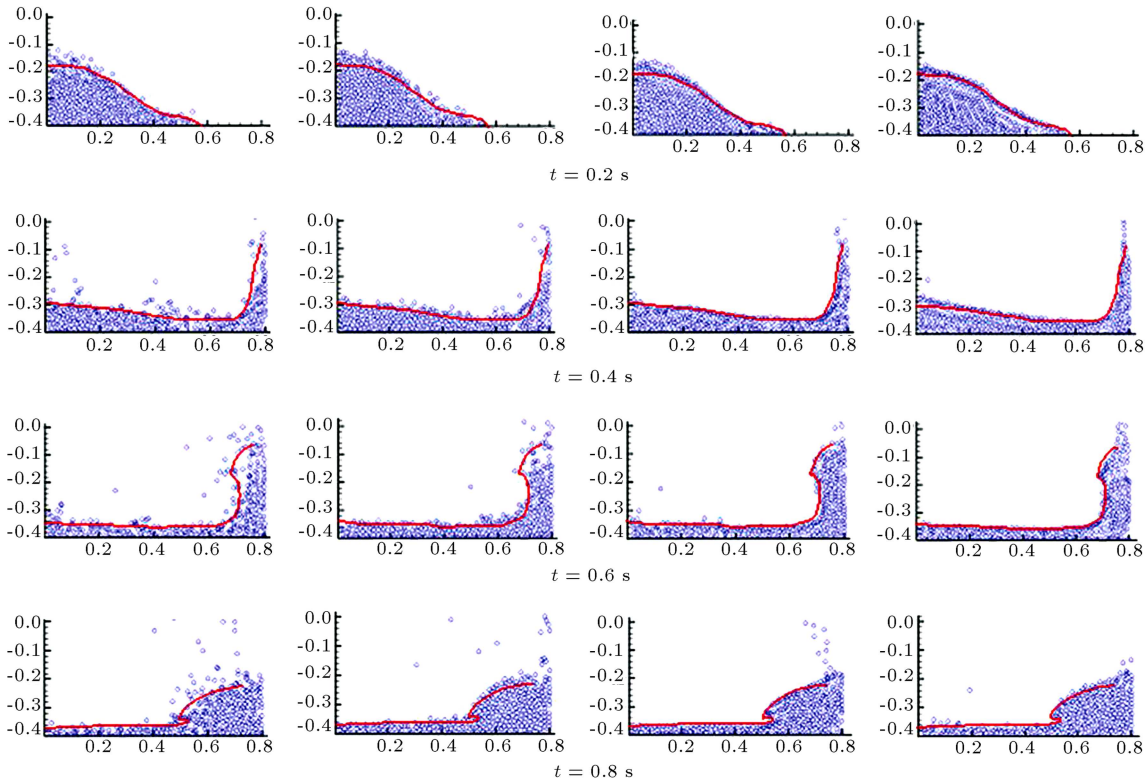

Figure 2. Comparison of model results at t= 0.2, 0.4, 0.6, 0.8 and 1 (s) after water column collapse with experimental results of Koshizuka (1996) [17]: a) Inviscid fluid; b) fluid with constant viscosity; c) Prandtl's mixing length theory; and d) $k-\varepsilon$ model.

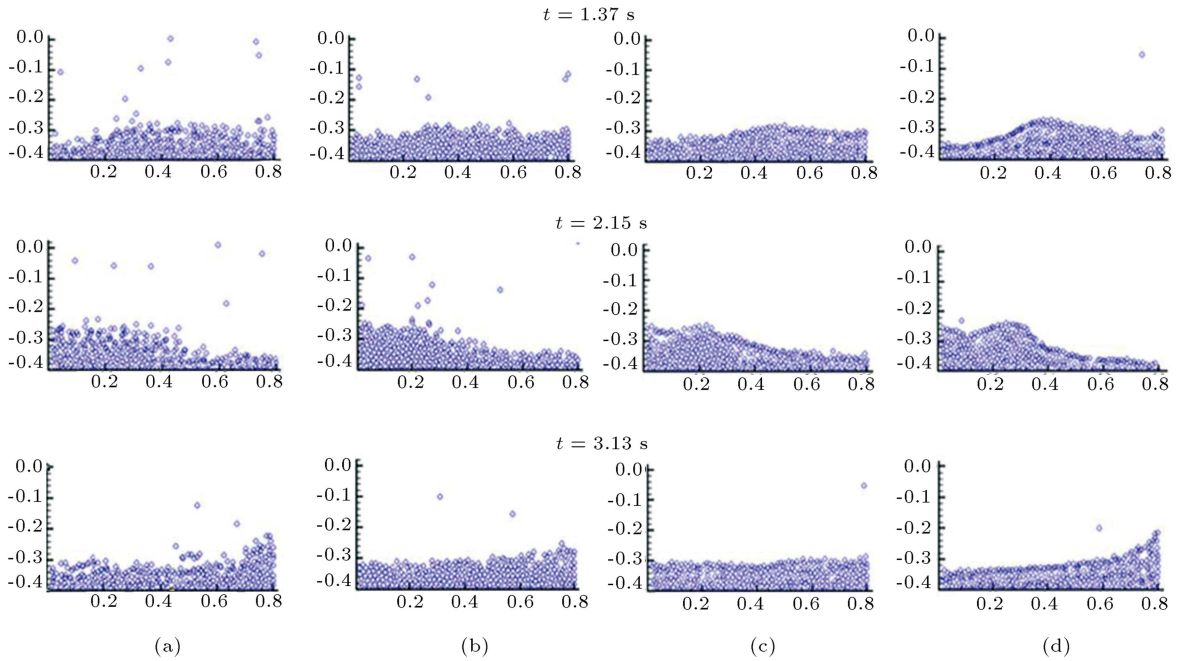

Figure 3. Model results at t= 1.37, 2.15, 3.13 (s) after water column collapse with results of a) inviscid fluid, b) fluid with constant viscosity, c) Prandtl's mixing length theory, and d) $k-\varepsilon$ model.

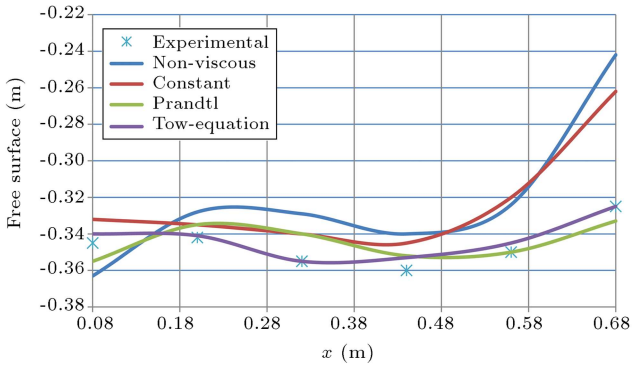

Figure 4. Comparison of free surfaces of different turbulent methods at $t = 0.6$ s.

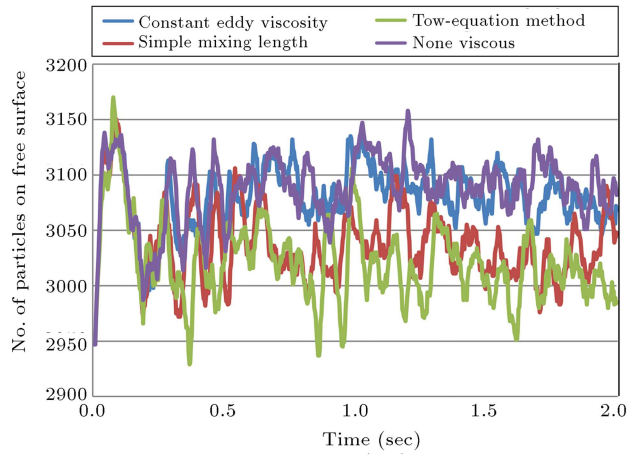

Figure 5. Results of number of free surface particles at different time steps for inviscid fluid, fluid with constant viscosity, Prandtl's mixing length theory and $k-\varepsilon$ model.

Table 2. Comparison between successful simulation time (s) for different kernel functions with different turbulence models.

$k-\varepsilon$	Prandtl's mixing length theory	Constant viscosity	Inviscid	Kernel function
>6	>6	1.4	1	KF1
>6	>6	>4	0.96	KF2
>6	>6	>4	1.4	KF3
>6	>6	2.6	0.95	KF4
>6	>6	0.95	0.8	KF5
>6	>6	>4	>4	KF6

function on stability of present model in presence of turbulence closures is investigated using six Kernel functions presented in Table 2.

According to Table 2, by using the Prandtl's mixing length theory and turbulence model, the developed MPS model is capable of modeling the dam break problem for more than 6 seconds. However, in lack of eddy viscosity, just by using the sixth Kernel function, KF6, the model can solve the dam break problem for approximately 4 seconds [19]. Thus, by enforcing the turbulence, the role of Kernel function in stability of MPS method (for the specified dam break problem) is disappeared. It is worth mentioning that for each of inviscid fluid, fluid with constant eddy viscosity, Prandtl's mixing length theory, and two-equation $k-\varepsilon$, a sensitivity analysis is carried out for efficient radius of Kernel functions.

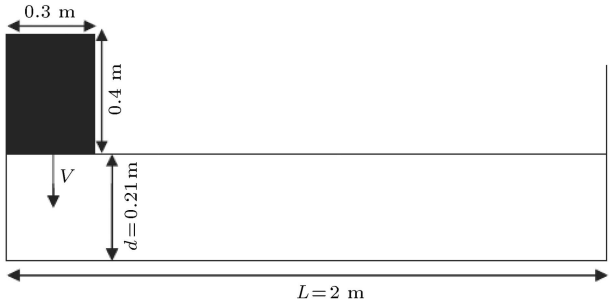

Figure 6. Initial condition of Scott Russell wave generator problem [31].

5.2. Scott Russell wave generator

In this section, solitary wave generated by a heavy box falling vertically into water tank is analyzed. Monaghan and Kos [15] examined this problem both experimentally and numerically using SPH method. Atai-Ashtiani and Shobeyri [33] simulated the problem using I-SPH method. In the current study, this problem is simulated with MPS method and is focused on the free surface modeling and the pressure field to demonstrate the effect of utilizing the new algorithm in solving Poisson equation.

The box had the width of 0.3 m and the height of 0.4 m. Three different water depths were considered in the experimental program. In this research study the case with 0.21 m water depth is chosen. The initial condition of the problem is shown in Figure 6. It should be noted that the horizontal length of the numerical tank is assumed to be 2 m, much shorter than that of the experimental tank, being 9 m. However the difference in the length of tank does not influence the results [33].

The vertical velocity of the box is expressed by [15]:

$$\frac{V}{\sqrt{d^D}} = 1.03\frac{Y}{D}\left(1-\frac{Y}{D}\right)^{0.5}, \qquad (33)$$

where D is the depth of water, Y is the height of the bottom of the box above the bottom of the tank at the time t, g is the acceleration due to gravity, and V is the falling vertical velocity of the box at time t.

The box sinks rapidly and the water beneath is forced out and upward. Then a reverse plunging wave forms and a solitary wave is initiated. The plunging wave collapses and produces a vortex which follows the solitary wave to the right hand side of the tank. The vortex goes forward to about 20 cm from the right of the box at 0.7 s in this study (Figure 7). Monaghan and Kos [15] reported that it has moved approximately 20 cm and Atai-Ashtiani and Shobeyri [33] declared the distance about 23 cm at the time 0.7 s.

In Figure 8, comparison of solitary wave profile obtained from developed numerical model with the

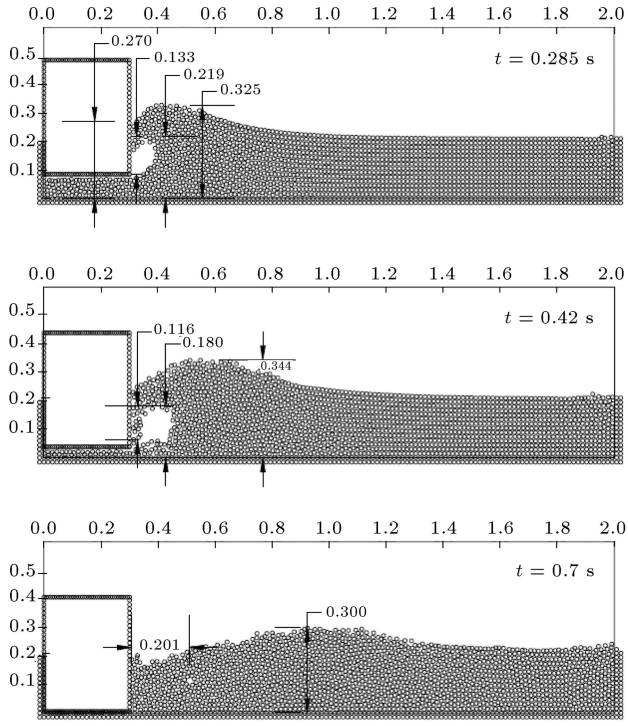

Figure 7. Particle configuration computed by the MPS model using $k-\varepsilon$ turbulence closure at times $t = 0.285$ s, $t = 0.42$ s, and $t = 0.7$ s for Scott Russell wave generator ($R = 0.013$ m).

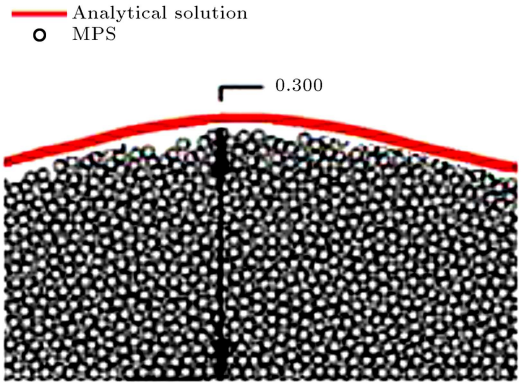

Figure 8. Comparison between wave profiles of analytical solution and present method for the wave generated by Scott Russell wave generator at $t = 0.7$ s ($R = 0.013$ m).

analytical solution of Scott Russell wave generator is presented. The wave amplitude was measured 9.2 cm in the experiment. Monaghan and Kos [15] reported the amplitude of 10.8 cm (SPH), while Atai-Ashtiani and Shobeyri [33] computed the wave amplitude 11 cm (I-SPH). In this study, the wave amplitude is 10.3 cm, which represent a more accurate value in compare with previous modeling results reported in the literature.

Figure 9 shows a number of characteristic lengths, measured at $t = 0.285$ s. The values of parameters are given in Table 3 for SPH, I-SPH, and MPS.

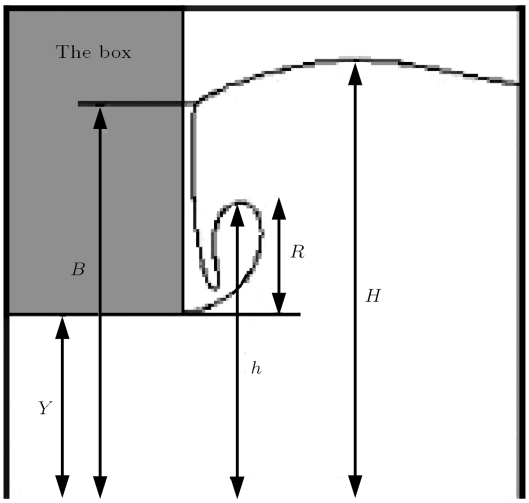

Figure 9. The definition of the Scott Russell wave generator problem at $t = 0.285$ s.

In Figures 10 and 11, the pressure field computed by developed MPS model is shown using with and without using ICCG method. It is seen that using ICCG increases the stability of the deployed method and decreases the pressure fluctuations.

5.3. Wave run-up and return

In this section, simulation of run-up and return of solitary wave on a beach collide a vertical wall is considered. Monaghan and Kos [14] performed the experiment and simulated this example using SPH method. The initial condition of the problem is shown in Figure 12. The solitary wave of the experiment was generated at one end by allowing heavily weighted box to drop to the bottom of the tank, such as the Scott Russell wave generator described in the previous section. The tank was 9 m long and 40 cm wide with initial water depth of 21 cm. The horizontal run of the ramp was 98 cm and the length of the horizontal section of the beach was 52 cm.

When the wave amplitude is sufficiently small, the Kortweg-De Vries equation shows that the height of the wave is given by [34]:

$$\eta = \frac{A}{\cos h^2 \left[\frac{x - Vt}{l}\right]}, \tag{34}$$

where x is distance parallel to the undisturbed surface, t is the time, A is the amplitude of incoming solitary wave, and l is the length scale for solitary wave which

Table 3. The comparison between length H, h, B and R computed by MPS method, I-SPH and SPH method, and experimental results.

Initial particle spacing	Method	Turbulence model	H(m)	R(m)	h(m)	B(m)
0.013	MPS	$k-\varepsilon$	0.325	0.133	0.219	0.27
0.013	MPS	Constant	0.319	0.1272	0.2056	0.27
0.015	MPS	Constant	0.315	0.125	0.197	0.265
0.015	I-SPH	-	0.329	0.13	0.218	0.255
0.01	I-SPH	-	0.3301	0.146	0.234	0.268
0.0042	SPH	-	0.3086	0.114	0.208	0.272
—	Experimental		0.333 ± 0.01	0.1333 ± 0.02	0.2273 ± 0.02	0.303 ± 0.02

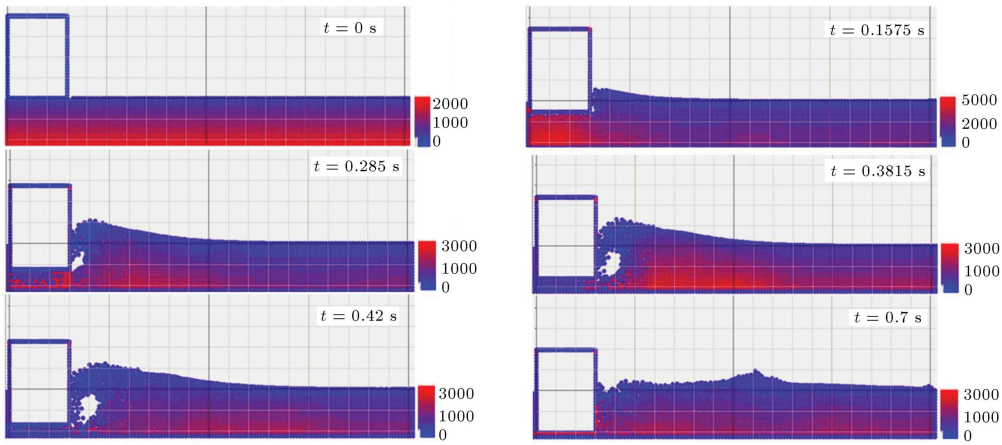

Figure 10. Pressure field computed by the present model using ICCG method at different times for Scott Russell wave generator problem.

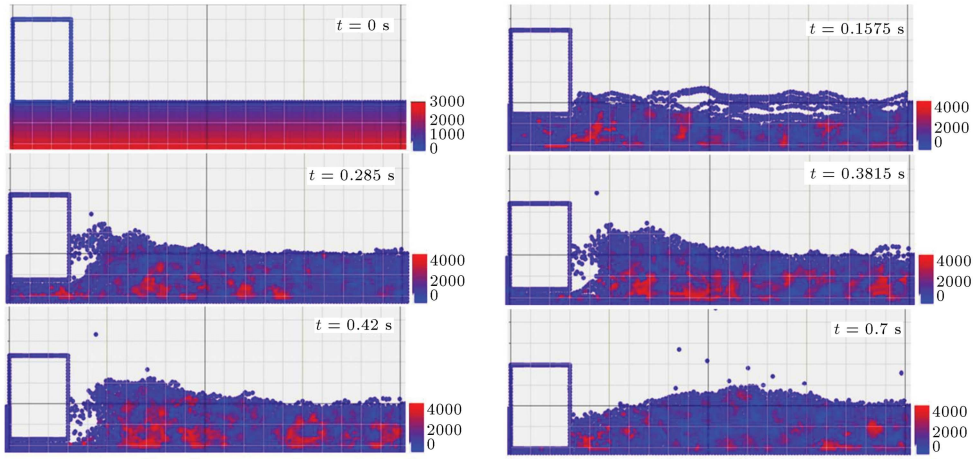

Figure 11. Pressure field computed by the present model without using ICCG method at different times for Scott Russell wave generator problem.

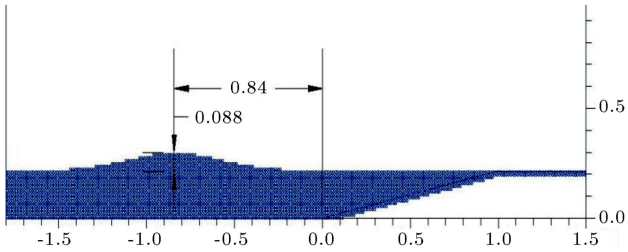

Figure 12. Initial conditions of MPS simulation of solitary wave run-up problem.

can be computed as:

$$l = \left(\frac{4D^3}{3A}\right)^{\frac{1}{2}}. \tag{35}$$

The speed of the wave V is given by:

$$V = \sqrt{gD}\left(1 + \frac{A}{2D}\right), \tag{36}$$

where D is the undisturbed water depth and g is gravitational acceleration.

Results obtained from the MPS model for generated wave are compared with Eqs. (35) and (36) for the wave length scale and wave speed. It is observed that computed wave length scale has 5% discrepancy while wave speed value has only 2% discrepancy from results obtained through Eqs. (35)-(36) [14]. Figure 13 shows the particle configuration computed by our model at different times for the current problem.

Monaghan and Kos [14] put the center of the solitary wave 84 cm to the left of the bottom edge of the ramp on their simulation and considered the length of the computation tank equal to 3.18 m. For their simulation the total number of particles was 12000.

In the current simulation, the solitary wave's center is set on 84 cm to the left of the bottom edge of

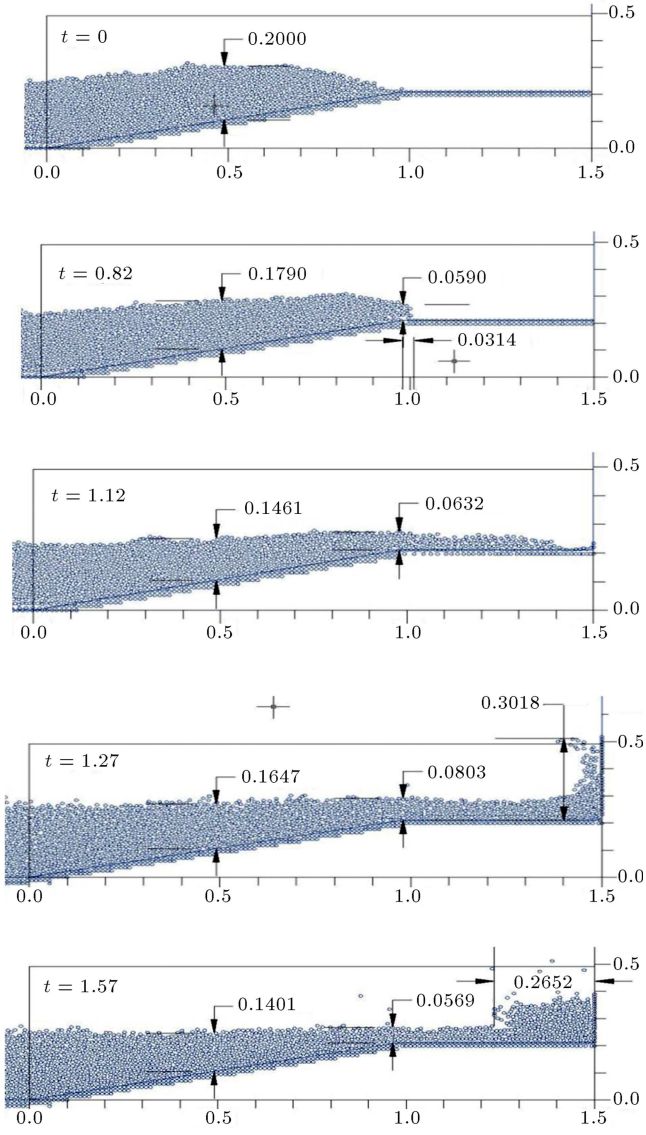

Figure 13. Particle configuration computed by the MPS model at times $t = 0$, 0.82, 1.12, 1.27, 1.57 s for wave run-up problem.

the ramp, too. The tanks length is assumed 3.3 m. The reference time, $t = 0$, is assumed to be at the moment when the solitary wave's peak is approximately halfway across the inclined section of the beach.

wave characteristic on and above slope are obtained through applying the developed model and compared with experimental results of Monaghan and Kos [14] in Table 4 based on parameters a, b and c defined in Figure 14.

According to the MPS model results, the maximum run of the wave is 0.3018 m for $t = 1.27$ s. Also the horizontal length of backed water, that is the distance between wave front and the vertical wall, is equal to 0.2652 m at time 1.57 s.

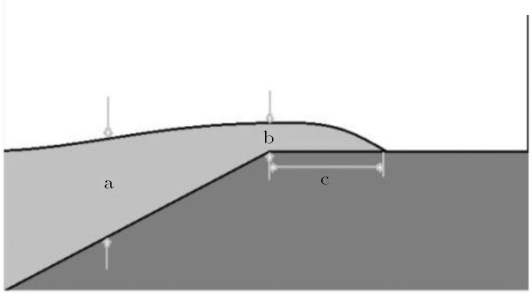

Figure 14. Definition of parameters of solitary wave run-up problem used in Table 4.

In Figures 15 and 16, the pressure field of wave run-up with and without using ICCG, are shown. The stability which was achieved through applying ICCG method is presented in these figures.

6. Conclusion

In this study, the effect of enforcing turbulence on the accuracy of the free surface flow estimation is investigated. Accuracy of the developed model was evaluated using a dam break problem which is solved numerically by moving particle semi-implicit method. Subsequently, the ICCG pressure algorithm is added to the MPS model to stabilize the solution procedure. The effect of utilizing ICCG which compute the pressure field implicitly, was shown via two test cases including Scott Russell wave generator and run up and return of a solitary wave.

Although the computational effort of model in case of inclusion of turbulence is more than the case of inviscid fluid or fluid with constant eddy viscosity, the comparison of results indicate that inclusion of turbulence closures in modeling complex free surfaces of two-dimensional turbulent flows tends to the more accurate results. The stability and accuracy of MPS model in modeling complex flow surfaces can be

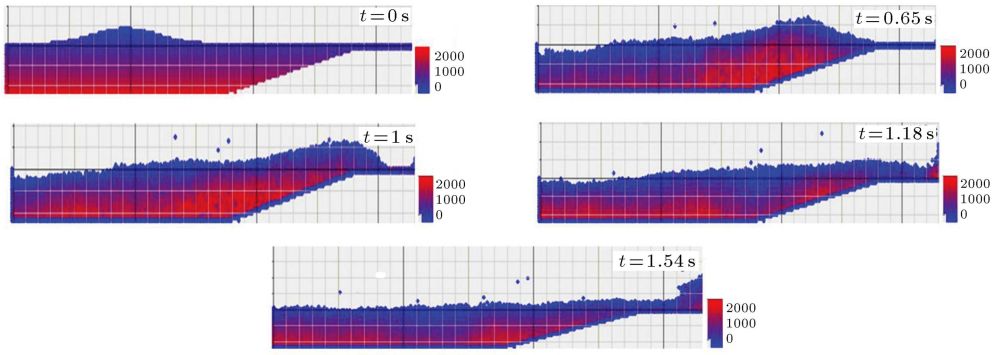

Figure 15. Pressure field computed by the MPS model using ICCG method at different times for wave run-up problem.

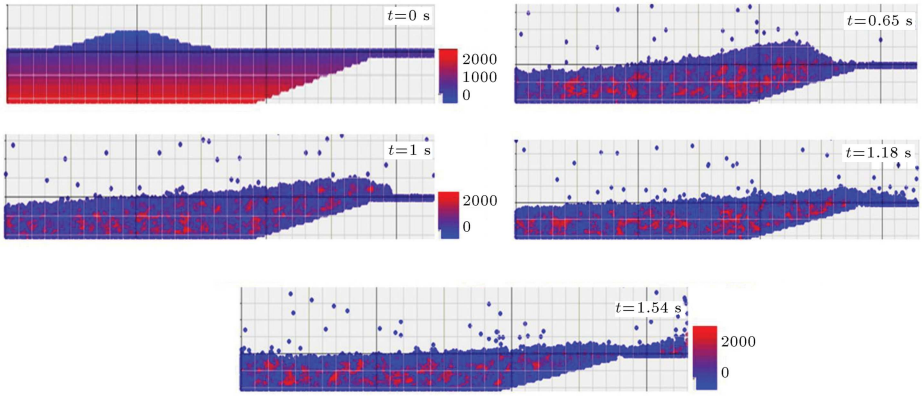

Figure 16. Pressure field computed by the MPS model without using ICCG method at different times for wave run-up problem.

Table 4. Comparison between parameters defined in Figure 13 in experiment and numerical simulations for different times.

MPS ($k-\varepsilon$ turbulence model)	t(s)				
	0	0.82	1.12	1.27	1.57
a	0.2	0.1790	0.1461	0.1647	0.1401
b	—	0.059	0.0632	0.0803	0.0569
c	—	0.0314	—	—	—
Experimental	t(s)				
	0	0.82	1.12	1.27	1.57
a	0.1970	0.1750	0.1409	0.1356	0.1409
b	—	0.045	0.0801	0.0700	0.045
c	—	0.0451	—	—	—

increased by considering turbulence. This can be achieved by implementing turbulence closures such as Prandtl's mixing length theory and two-equation $k-\varepsilon$ for calculating eddy viscosity and location of particles. Moreover, by enforcing the turbulence the type of Kernel function will be no longer has effect on the stability of MPS method in modeling dam break problem and therefore any kernel function can be deployed for modeling purposes. Consequently, by determining eddy viscosity of particles in each time step using turbulence closures, the modeling duration could be enlarged to more than 6 seconds for all applied Kernel function which is a major improvement in compare with previous models developed in the area of dam break problem predictions.

To confirm the above conclusion for the other complex free surface flow simulation, results obtained through MPS model incorporating $k-\varepsilon$ turbulence closure were applied to additional test cases and compared with experimental measurement as well as other numerical model results cited in the literature. In all cases it was found that applying turbulence closure model can improve the stability of the simulation as well as the accuracy of results.

References

1. Ashgriz, N. and Poo, J.Y. "Flux line-segment model for advection and interface reconstruction", *J. of Comput. Phys.*, **93**, pp. 449-468 (1991).
2. Van der Meer, J.W., Petit, H.A.H., Van den Bosch, P., Klopman, G. and Broekens, R.D. "Numerical simulation of wave motion on and in coastal structures", *23rd Int. Conf. on Coastal Engrg.*, Venice, Italy, ASCE, **2**, pp. 1772-1784 (1992).
3. Hieu, P.D. and Tanimoto, K. "A two-phase flow model for simulation of wave transformation in shallow water", *4th Int. Summer Symposium*, Kyoto, Japan, JSCE, pp. 179-182 (2002).
4. Lucy, L.B. "A numerical approach to the testing of the fission hypothesis", *Astron. J.*, **82**(12), pp. 1013-1024 (1977).
5. Gingold, R.A. and Monaghan, J.J. "Smoothed particle hydrodynamics: Theory and application to non-spherical stars", *Monthly Notices of the Royal Astronomical Society*, **181**, pp. 375-389 (1977).
6. Monaghan, J.J. "Smoothed particle hydrodynamics", *Annual Review of Astronomy and Astrophysics*, **30**, pp. 543-574 (1992).
7. Libersky, L.D., Petschek, A.G., Carny, T.C., Hipp, J.R. and Allahdady, F.A. "High strain lagrangian hydrodynamics a three-dimensional (SPH) code for dynamic material response", *J. Comput. Phys.*, **109**, pp. 67-75 (1993).
8. Randles, P.W. and Libersky, L.D. "Smoothed particlehydrodynamics: Some recent improvements and applications", *Comput. Meth. Appl. Mech. Engrg.*, **138**, pp. 375-408 (1996).
9. Monaghan, J.J. "Implicit SPH drag and dust dynamics", *J. Comput. Phys.*, **138**, pp. 801-820 (1997).
10. Gomez-Gesteira, M.D., Rogers, B., Dalrymple, R.A., J.C. and Crespo, A. "State-of-the-art of classical SPH for free-surface flows", *J. of Hydraul. Res.*, **48** (extra issue), pp. 6-27 (2010).
11. Monaghan, J.J. "Simulating free surface flows with SPH", *J. Comput. Phys.*, **110**, pp. 399-406 (1994).
12. Monaghan, J.J. "Gravity currents and solitarywaves", *Phys*, **98**, pp. 523-533 (1996).
13. Monaghan, J.J., Cas, R.A.F., Kos, A.M. and Hallworth, M. "Gravity currents descending a ramp in a stratified tank", *J. Fluid Mech.*, **379**, pp. 39-70 (1999).
14. Monaghan, J.J. and Kos, A. "Solitary wave on a Cretan beach", *J. of Waterway, Port, Coastal and Ocean Engineering, ASCE*, **125**(3), pp. 145-154 (1999).
15. Monaghan, J.J. and Kos, A. "Scott Russell's wave generator", *Phys. Fluids*, **12**(3), pp. 622-630 (2000).
16. Fang Parriaux, J., Rentschler, M. and Ancey, C. "Improved SPH methods for simulating free surface flows of viscous fluid", *Appl. Num. Math.*, **50**, pp. 251-271 (2008).

17. Koshizuka, S. and Oka, Y. "Moving particle semi-implicit method for fragmentation of incompressible fluid", *Nucl. Eng. Sci.*, **123**, pp. 421-34 (1996).

18. Khayyer, A. and Gotoh, H. "Development of CMPS method for accurate water surface tracking in breaking wave", *Coast. Eng.*, **50**(2), pp. 179-207 (2008b).

19. Atai-Ashtiani, B. and Farhadi, L. "A stable moving-particle semi-implicit method for free surface flows", *Fluid Dyn. Res.*, **38**, pp. 241-256 (2006).

20. Khayyer, A. and Gotoh, H. "Enhancement of stability and accuracy of the moving particle semi-implicit method", *J. Comput. Phys.*, **230**, pp. 3093-3118 (2011).

21. Kondo, M. and Koshizuka, S. "Improvement of stability in moving particle semi-implicit method", *Int. J. Numer. Meth. in Fluids*, **65**(6), pp. 638-654 (2010).

22. Suzuki, Y. and Koshizuka, S. "Hamiltonian Moving-Particle Semi-implicit (HMPS) method for incompressible fluid flows", *Comput. Methods Appl. Mech. Engrg*, **196**, pp. 2876-2894 (2007).

23. Shao, S.D. and Gotoh, H. "Turbulence particle models for tracking free surfaces", *J. of Hydraul. Res.*, **43**(3), pp. 276-289 (2005).

24. Tian, W., Ishiwatari, Y., Ikejiri, S., Yamakawa, M. and Oka, Y. "Numerical simulation of thermally controlled steam bubble condensation using moving particle semi-implicit (MPS) method", *Ann. of Nucl. Energy*, **37**, pp. 5-15 (2010).

25. Shibata, K. and Koshizuka, S. "Numerical analysis of shipping water impact on a deck using a particle method", *Ocean Eng.*, **34**, pp. 585-593 (2007).

26. Shakibaeinia, A. and Jin, Y.C. "A weakly compressible MPS method for simulation openboundaryfree-surface flow", *Int. J. Numer. Meth. in Fluids*, **63**(10), pp. 1208-1232 (2010).

27. Akimoto, H. "Numerical simulation of the flow around a planning body by MPS method", *Ocean Eng.*, **64**, pp. 72-79 (2013).

28. Fayyaz, M. and Kolahdouzan, M. "Free surface modeling of flow by MPS method", *8th Int. Cong. on Civil Engrg.*, Shiraz, Iran (2009).

29. Violeau, D. and Issa, R. "Numerical modeling of complex turbulent free-surface flows with the SPH method: and overview", *Int. J. for Numer. Meth. in Fluids*, **53**, pp. 277-304 (2006).

30. Li, W. and Lam, S. *Principles of Fluid Mechanics*, Addison - Wesley Publishing company (1964).

31. Shao, S.D. and Lo, E.Y.M., "Incompressible SPH method for simulating Newtonian and non-Newtonian flows with a free surface", *Adv. Water Resour.*, **26**(7), pp. 787-800 (2003).

32. Rodi, W. "Turbulence models and their application in hydraulics-A state of the art review", *Int. Association for Hydraulic Research*, Delft, Netherland (1980).

33. Atai-Ashtiani, B. and Shobeyri, G. "Numerical simulation of landslide impulsive waves by incompressible smoothed particle hydronamics", *Int. J. for Numer. Meth. in Fluids*, **56**, pp. 209-232 (2008).

34. Lamb, H. *Hydrodynamics*, Cambridge Univ. Press, Cambridge, U.K. (1932).

Biographies

Morteza Kolahdoozan, PhD, received his BSc from the department of Civil Engineering, Amirkabir University of Technology, MSc from the Department of Civil Engineering, Tehran University and PhD from the University of Bradford, UK. He is currently a faculty member at the department of Civil and Environmental Engineering, Amirkabir University of Technology, Tehran, Iran. His research interests include Fluid mechanics, coastal hydrodynamics and sediment transport, water quality evaluation, numerical and physical modeling of coastal, estuarial and riverine phenomena. He has long term collaboration on research projects with industry and also is senior consultant of a number of governmental bodies namely Ministry of Energy and Ministry of transportation. He is also a member of Iranian society of hydraulic association and Iranian society of Marine engineers.

Mina Sadat Ahadi, MSc, received her BSc in Water Engineering from Gilan University and her MSc in Hydraulic Engineering from Amirkabir University of Technology, Tehran, Iran. She has worked on numerical modeling of sediment transport using a method called Moving Particle Semi-implicit by developing a code in Fortran programming language. Her research interests include computational fluid dynamics, multiphase flows, and sediment transport. She has been working as a researcher and hydrodynamic modeler at Pouya Tarh Pars Consulting Engineers Co. She is also a member of Iranian National Committee on Irrigation and Drainage (IRNCID) from 2005.

Samina Shirazoor, MSc, received her BSc in Civil Engineering from Shahid Bahonar University of Kerman and her MSc in Hydraulic Engineering from Amirkabir University of Technology, Tehran, Iran. She has worked on numerical modeling of free surface flow using a Lagrangian meshless method called moving particle semi-implicit by developing a code in Fortran programming language. Her research interests include estimating free surface flow considering the effect of turbulence, multi-phase flows and floating breakwater. She is working as a lecturer of hydraulic at Shahid Bahonar University (Kerman) and also as a Civil engineer at Chehel Ashkoob consulting engineer, Amoodan consulting engineer and Faza Raz consulting engineer.